JOURNAL OF MATERIALS SCIENCE: MATERIALS IN MEDICINE **16** (2005) 873–879

Biomimetic mineralization of partially bioresorbable glass fiber reinforced composite

M. VÄKIPARTA[1,*], A.-P. FORSBACK[2], L. V. LASSILA[3], M. JOKINEN[4], A. U. O. YLI-URPO[3], P. K. VALLITTU[3]
[1]*University of Turku, Institute of Dentistry, Department of Prosthetic Dentistry, Turku Biomaterials Centre, Itäinen Pitkäkatu 4 B, FIN-20520 Turku, Finland*
E-mail: marju.vakiparta@utu.fi
[2]*University of Turku, Institute of Dentistry, Turku Biomaterials Centre, Turku, Finland*
[3]*University of Turku, Institute of Dentistry, Department of Prosthetic Dentistry and Biomaterials Research, Turku, Finland*
[4]*University of Turku, Institute of Dentistry, Department of Prosthetic Dentistry, Turku Biomaterials Centre, Turku, Finland*

The aim of this study was to investigate the biomimetic mineralization on the surface of a glass fiber reinforced composite with partially resorbable biopolymer matrix. The E-glass fibers were preimpregnated with a novel biopolymer of poly(hydroxyproline) amide, and further impregnated in the monomer system of bis-phenyl glycidyl dimethacrylate (Bis-GMA)—triethylene glycol dimethacrylate (TEGDMA), which formed interpenetrating polymer networks (IPN) with the preimpregnation polymer. After light-initiated polymerization of the monomer system, the rhombic test specimens ($n = 6$) were immersed in the simulated body fluid (SBF) with the bioactive glass for 24 h, and then the apatite nuclei were allowed to grow for 1, 3, 5 and 7 days in the SBF. The control test specimens ($n = 3$) were immersed in SBF without the bioactive glass. According to the scanning electron microscope (SEM), a mineral layer was formed on the surface of all the specimens, which were immersed with bioactive glass. The layer was thickened by the prolonged immersion time to a uniform layer. The Ca/P atomic ratio of the mineral varied between 1.30 and 1.54 as analyzed by the energy dispersive X-ray analysis (EDXA). The Fourier transform infrared spectroscopy (FT-IR) spectra gave signals for the mineral, which are characteristic of both bone-like apatite and orthocalciumphosphate. In conclusion, the mineral layer was formed on the surfaces of the specimens by biomimetic mineralization, the mineral being a mixture of bone-like apatite, orthocalciumphosphate and other calcium phosphates.

1. Introduction

It has been suggested that the essential requirement for an artificial material to bond to living bone is the formation of a layer of biologically active carbonate-containing apatite on the surface of the material [1, 2]. On the surface of sol-gel-prepared silica gels and bioactive glasses or glass ceramics, a bioactive apatite layer can be spontaneously formed *in vitro* [3–5] and *in vivo* [6, 7]. When the apatite nuclei are formed, they grow by taking calcium and phosphate ions from the surrounding fluid, thus forming a dense, uniform layer of the apatite on the surface of the material. The apatite layer can also be formed on the surfaces of metals [8] or polymers [9–11] in the presence of a silica source or, in some cases, even without it [12]. The formation of the apatite layer *in vitro* in the test tube, so-called biomimetic mineralization, is believed to mimic the formation of the apatite layer *in vivo*, and is thought to describe the bioactivity of the material. In this process described by Kokubo [8–10], a substrate is placed in the same tube along with the silica source, for example, SiO_2-based glass particles, and soaked in the simulated body fluid (SBF) with an ion concentration almost equal to human blood plasma at body temperature.

Non-resorbable polymers have specific applications in the field of medicine; they are used, for example, as orthopedic bone cements or as a part of implants [13, 14]. In dentistry, the non-resorbable polymers have been used for decades as prosthetic material. In these applications, a polymethyl methacrylate (PMMA) powder is mixed with, e.g. methylmethacrylate-ethylene glycol dimethacrylate monomers [15]. By free radical polymerization, an interpenetrating polymer network (IPN) structure for multiphase polymer is formed. By

*Author to whom all correspondence should be addressed.

definition, the IPN is formed from the linear polymer, which is partially or totally dissolved probably by bi- or multifunctional monomers [16]. On completion of the polymerization, a cross-linked interphase, called IPN is formed, between the linear phase and the matrix. A polymer structure of this kind has been successfully used as matrix polymer for dental fiber-reinforced composites (FRC) [17, 18].

A recent development in bioresorbable polymers has produced a new type of polymer such as biodegradable poly(hydroxyproline) [19], which has been described as non-toxic in *in vitro* conditions [20]. The oligomer form of poly(hydroxyproline) has the ability to produce porosity in the acrylic bone cement in a moist environment, providing an opportunity for bone ingrowth *in vivo* [21, 22]. Interest has been shown in combining non-resorbable and resorbable polymers in the form of IPN for fiber-reinforced composites. The bioresorbable polymer has been used in coating, i.e. so-called sizing, the reinforcing fiber and combining it with the non-resorbable polymer. The structure of a polymer matrix of this kind allows canal formation between the fibers on the non-resorbable polymer matrix. It could be hypothesized that bone ingrowth can occur into the canals. By using the partially resorbable fiber-reinforced composite in orthopaedic applications, it is possible to decrease the stress concentrations at the interface of the implant and the bone. Bone ingrowth into the composite canals transfers stress from the interface to the inside of the composite near to the reinforcing fibers where the bone can be in direct contact with the fibers. Dissolution of the bioresorbable polymer after implantation weakens the mechanical properties of the composite temporarily until the bone has grown into the open canals. However, the reinforcing fibers in the composite might be able to maintain the mechanical strength of the composite at the required level in the potential application, such as in a load-bearing dental or orthopaedic implant made of FRC.

The aim of the study was to investigate the biomineralization on the surface of the experimental, partially resorbable fiber-reinforced composite. The rate of formation of the mineral layer was investigated morphologically and qualitatively by SEM-EDX analysis. The molecular composition of the formed mineral was examined with FT-IR spectroscopy utilizing a diffuse reflectance (DRIFT) system.

2. Materials and methods

2.1. Polymers

The experimental linear and solid bioresorbable biopolymer of poly(4-hydroxy-L-proline) amide (PA) (Fig. 1) was synthesized by the melting condensation polymerization method as described by Puska *et al.* [21]. Trans-4-hydroxy-L-proline was converted into an ester by esterification and, after that, the isolated and purified monomer was subjected to melt-polycondensation at elevated temperatures in vacuo. The molecular weight of the polymer was controlled by the polymerization process. In this study, the molecular weight of the PA was 2.200 g/mol. For test specimen fabrication, a solution of PA was made by adding the solvent trifluoroethanol (TFE) until the polymer concentration was 50 mg/ml.

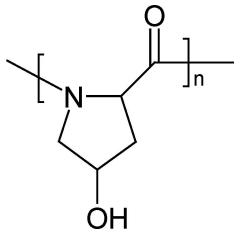

Figure 1 The structure of poly(4-hydroxy-L-proline) amide.

The bifunctional monomer resin system was prepared by mixing the bis-phenyl glycidyl dimethacrylate (Bis-GMA) and the triethylene glycol dimethacrylate (TEGDMA) in the ratio 70:30. Next, 0.14 g of activator dimethyl amino ethyl methacrylate (DMAEMA) (0.35 wt%) was mixed with 0.15 g of the light polymerization initiator camphorquinone (0.35 wt%) to obtain the monomer system for the non-resorbable phase of the polymer matrix. Thus, 11.72 g of TEGDMA (29.3 wt%) was added to the mixture and it was stirred. Finally, 28.00 g of Bis-GMA (70 wt%) was added.

2.2. Fabrication of test specimen

Six different test groups (see Table I) were investigated in this study. There were six rhombic specimens (size 2 mm × 2 mm × 4 mm) in the groups (BN, BEN and BESN), which were treated with bioactive glass (defined below) and three in the groups (BK, BEK and BESK) which were not treated with bioactive glass.

Continuous unidirectional E-glass fiber (diameter of individual fibers: 14 μm) rovings (composition: SiO_2 55%, CaO 22%, Al_2O_3 15%, B_2O_3 6%, MgO 0.5% and Fe + Na + K less than 1.0%), which were silanized (process R332, Ahlström, Karhula, Finland) were preimpregnated with the PA in the TFE solution. After evaporation of the solvent, the fiber rovings were further impregnated with the Bis-GMA-TEGDMA monomer system. The further impregnation time was 24 h and it was carried out in a dark chamber. The fiber rovings were placed parallel to each other into

TABLE I Description and classification of test groups

Group	Description
BN	Bis-GMA[a]–TEGDMA[b]–matrix, treated with bioactive glass
BK	Bis-GMA–TEGDMA–matrix, not treated with bioactive glass
BEN	Glass fibers[c] + Bis-GMA–TEGDMA–matrix, treated with bioactive glass
BEK	Glass fibers + Bis-GMA–TEGDMA–matrix, not treated with bioactive glass
BESN	Glass fibers with PA[d] preimpregnation + Bis-GMA–TEGDMA–matrix, treated with bioactive glass
BESK	Glass fibers with PA preimpregnation + Bis-GMA–TEGDMA–matrix, not treated with bioactive glass

[a]bis-phenyl glycidyl dimethacrylate.
[b]triethylene glycol dimethacrylate.
[c]E-glass, continuous unidirectional, diameter 14 μm.
[d]poly(trans-4-hydroxy-L-proline) amide.

the stainless steel molds (size 2 mm × 2 mm × 25 mm) with an excess of the monomer resin system. The molds were covered with mylar film and glass plates. The specimens were initially polymerized with an Elipar^{TM} Highlight (Espe, Seefeld, Germany) light-polymerization unit (wavelength 480 nm, light intensity ca 600 mW/cm^2) for 40 s from both sides. After the initial polymerization, the specimens were post-cured with a light-curing device (LicuLite, Dentsply DeTrey GmbH, Dreieich, Germany) for 15 min. During the post-curing, temperature rose to 80 °C. The specimens were cut perpendicularly in to the fiber direction to the test specimen size of 2 mm × 2 mm × 4 mm with a hand-held micromotor bur with a diamond disc (Komet Miniflex 945B, GERB. BRASSELER GmbH, Lemgo, Germany). The specimens for the biomimetic mineralization were made by wet grinding the surface of the specimens with silicone carbide grinding paper (SiC, FEPA P #4000, Struers).

2.3. Biomimetic mineralization

The mineral formation was studied *in vitro* using simulated body fluid (SBF). The SBF was prepared by dissolving the chemical reagents of NaCl, $NaHCO_3$, KCl, $K_2HPO_4 \times 3H_2O$, $MgCl_2 \times 6H_2O$, $CaCl_2$ and Na_2SO_4 in deionized water as shown in Table II [4]. The solution was buffered at physiological pH 7.4 (37 °C) with tris(hydroxymethyl aminomethane) and hydrochloric acid.

A bioactive glass S53P4 (BAG; Na_2O 23%, CaO 20%, P_2O_5 4%, SiO_2 53%, Abmin Technologies Ltd., Turku, Finland) was used as the source of silica in the biomimetic process. The glass was used as powder with a particle size of <45 μm.

The biomimetic method described earlier [8–10] was modified using 1.0 SBF in this study instead of the commonly used 1.5 SBF. The 1.0 SBF is preferred because it corresponds to the inorganic part of real body fluid and shows better the material's ability to nucleate calcium phosphate on its surface. In 1.5 SBF, for example, the calcium concentration is so high (1.5 times that of real body fluid) that calcium phosphate is formed almost on any surface present in the system and even homogeneous nucleation is possible in the metastable system. The CaP formation was examined on the surface of test specimens after treatment with the BAG in the SBF described above.

TABLE II Reagents for preparing the SBF and ion concentrations of SBF and human plasma

				Concentration (mM)	
Order	Reagent	Amount/1l (H_2O)	Ion	Simulated fluid	Human plasma
1	$(CH_2OH)_3CNH_2$	6.241 g			
2	NaCl	7.995 g	Na^+	142.0	142.0
3	$NaHCO_3$	0.353 g	K^+	5.0	5.0
4	KCl	0.224 g	Mg^{2+}	1.5	1.5
5	$K_2HPO_4 \times 3\ H_2O$	0.228 g	Ca^{2+}	2.5	2.5
6	$MgCl_2 \times 6\ H_2O$	0.305 g	Cl^-	147.8	103.0
7	$CaCl_2$	0.368 g	HCO_3^-	4.2	27.0
8	Na_2SO_4	0.071 g	HPO_4^{2-}	1.0	1.0
9	Trizma Base	1.259 g	SO_4^{2-}	0.5	0.5

The test specimens BN, BEN and BESN were first treated with 30 ml SBF buffer supplemented with 30 mg of the BAG at 37 °C for 24 h and then moved to another sample tube with 30 ml SBF at the same temperature for 1, 3, 5 and 7 days under continuous shaking. The SBF was changed every second day in order to sustain the calcium and phosphorus concentration at the level of human plasma because the concentrations of these ions decrease in time due to the nucleation and growth of calcium phosphate on the surface of the specimens. The other specimens, i.e. the controls (BK, BEK and BESK) were also incubated with 30 ml SBF for 1, 3, 5 and 7 days at 37 °C but not treated with the bioactive glass. After the given soaking period, the test specimens were removed from the fluid, gently washed twice with deionized water, and dried at 50 °C for 24 h.

2.4. SEM-EDX analysis

The morphology and the chemical composition of the surface of the specimens were examined using a scanning electron microscope (SEM, JEOL, Model JSM-5500, Tokyo, Japan) connected to an energy dispersive X-ray analyzer (EDXA, Princeton Gamma-Tech, Prism 2000, Princeton, New Jersey, USA). The analysis of the atomic ratio of the calcium and the phosphorus (Ca/P) in the precipitation on the surface of the test specimens was done using the Spirit X-ray Microanalysis System. The analysis was done on three distinct parts of the surface of the test specimens and the Ca/P values were taken on the mean of these. The thickness of the mineral layer was evaluated using line section analysis of the cross-sectional SEM images. The specimen was turned 90 degrees in the SEM vacuum chamber to evaluate the thickness of the mineral layer. The surfaces of the cross-sections of the test specimens were sputtered (Sputter coater BAL-TEC SCD 050, Balzers, Liechtenstein) with carbon for the SEM-EDX monitoring. A powder of commercial hydroxyl apatite (HA, $Ca_{10}(PO)_4(OH)_2$, J.T. Baker Chemical Co., Phillipsburg, USA) was compressed to the shape of a tablet using a hydraulic press (Perkin Elmer, Beaconsfield, England) before the EDX analysis. The Ca/P ratios of the specimens and tricalcium phosphate (TCP, $Ca_3(PO_4)_2$, J.T. Baker Chemical Co., Deventer, Holland) are scaled with relation to the Ca/P ratio of HA.

2.5. FT-IR analysis

The molecular composition and the structure of the mineral precipitates were investigated by Fourier transform infrared spectroscopy (FT-IR, Spectrum One, Instrument serial number 52434, Perkin Elmer, Beaconsfield, England) using a diffuse reflectance unit (DRIFT, accessory serial number 181296, Perkin Elmer, Beaconsfield, England). The spectra were recorded in the 400–4000 cm^{-1} range and at 2 cm^{-1} resolution averaging 32 scans. The IR spectra of the precipitate were compared with the spectra of pure commercial powder of HA and TCP, which was not immersed in SBF.

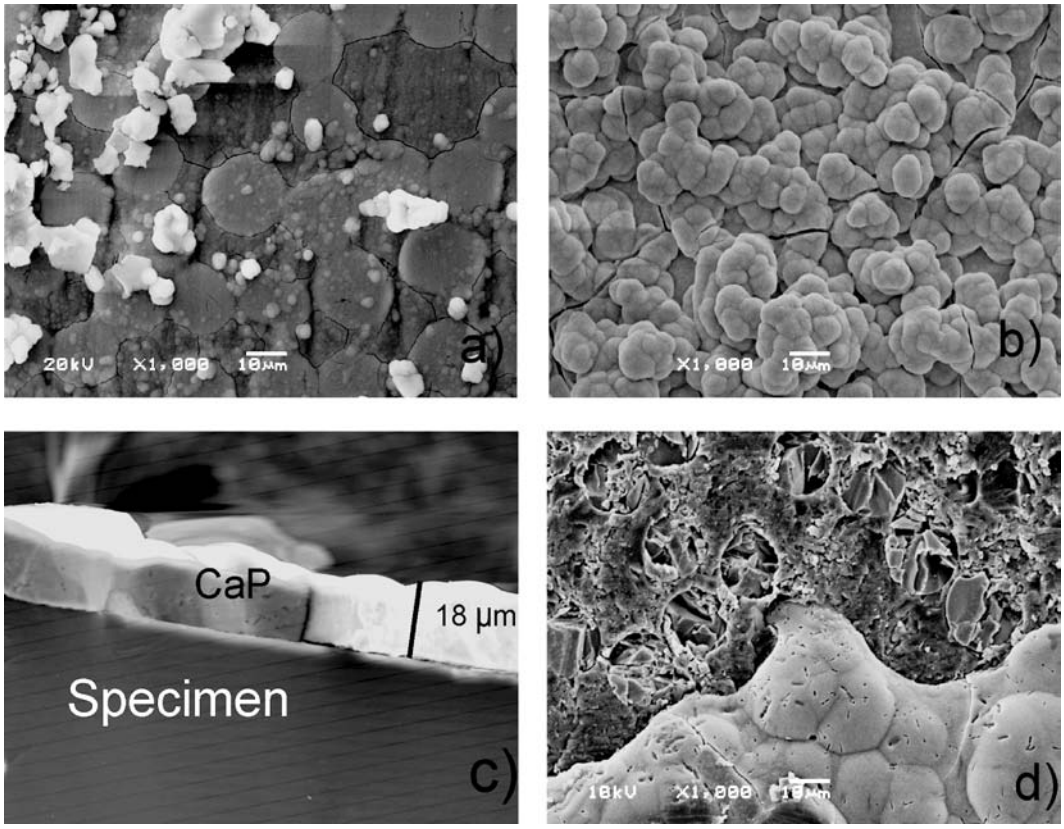

Figure 2 SEM photomicrographs of (a) BEN immersed in SBF for 1 day, (b) BN immersed in SBF for 3 days, (c) the thickness of the precipitation on the surface of the BESN after 7 days' immersion in SBF and (d) BESN immersed in SBF for 7 days (original magnification 1000x; bar = 10 μm for a, b and d).

3. Results

3.1. SEM

A thin layer of the precipitation of the mineral formed on the surface of BN, BEN and BESN after an immersion time of one day in SBF (BEN in Fig. 2(a)). With the longer immersion time, the mineral layer became thicker and covered the entire surface of the specimen (such in the case of BN immersed in SBF for three days; Fig. 2(b)), until it was about 18 μm thick at 7 days (for example BESN in Fig. 2(c)). The minerals seemed to penetrate into the open canals formed by the dissolution of the PA (Fig. 2(d): BESN immersed in SBF for 7 days). The test specimens (BK, BEK, and BESK; see Table I) in the control SBF, i.e. without bioactive glass, did not show mineral formation.

3.2. EDX analysis

A histogram of the calcium-phosphorus ratio (±SD) in the mineral layer on the surface of specimens is shown in Fig. 3. The Ca/P ratio in the precipitation on the surface of BN varied between 1.38 (±0.11) and 1.54 (±0.10) depending on the time point, while the Ca/P ratio for BEN varied between 1.37 (±0.03) and 1.53 (±0.06). For BESN, the Ca/P ratio varied between 1.31 (±0.03) and 1.48 (±0.04). Commercial HA and TCP, which was not treated with bioactive glass or immersed in SBF, were used as a reference for hydroxyl apatite (Ca/P = 1.68 ± 0.01 and 1.57 ± 0.04, respectively).

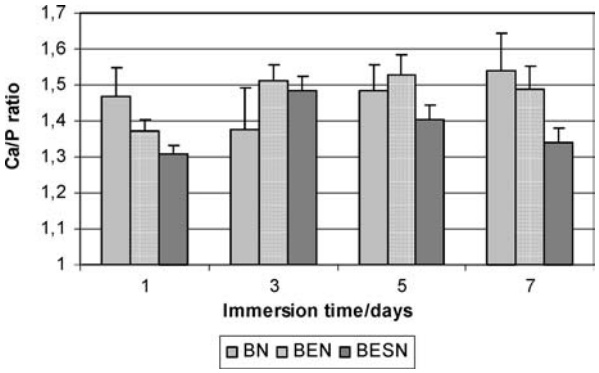

Figure 3 The atomic ratios of the Ca/P on the surface of the test specimens immersed in SBF for 1, 3, 5 and 7 days.

3.3. FT-IR analysis

Fig. 4 shows DRIFT FT-IR spectra of the precipitation on the surface of the specimens immersed in SBF for 0, 3, 5 and 7 days including FT-IR spectra of commercial pure and not-immersed TCP and HA. Hydroxyl stretch was observed at 3571 cm^{-1} and 630 cm^{-1} in the spectra of both the commercial HA and TCP. These hydroxyl bands were not detected in the specimens. On the test specimen's surface, there was a broad band in the 3700–2700 cm^{-1} ranges that resulted from water absorbed on to the mineral layer. The band at 1725 cm^{-1} was observed at the time points 0, 3 and 5 days but not at the 7 days and TCP and HA. The band at 1634 cm^{-1} could be assigned to a water or carbonate group. Two bands at 1449 and 1415 cm^{-1} resulted from carbonate groups (ν_3) incorporated in the calcium phosphate structure.

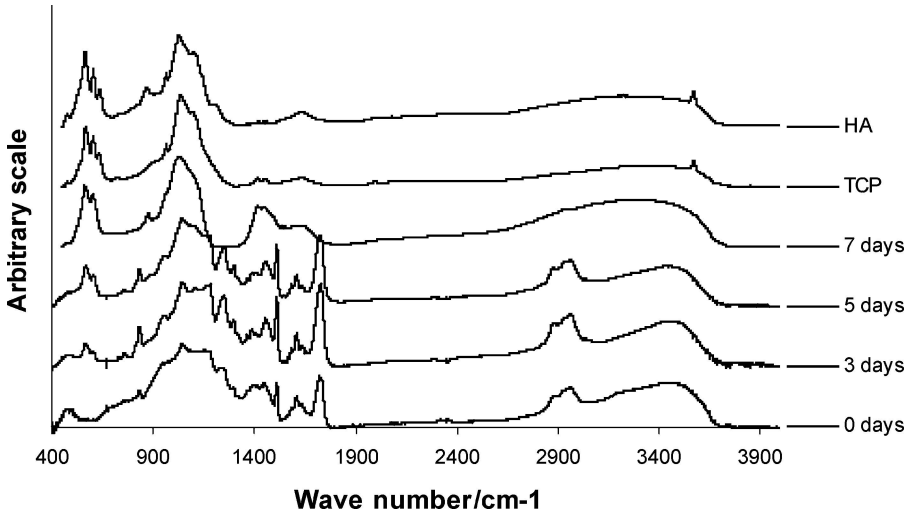

Figure 4 FT-IR spectra of the precipitation formed on the surface of the specimens as a function of immersion time in SBF (0 days: BEK, 3 and 5 days: BEN and 7 days: BN). Also the FT-IR spectra of TCP and HA are included to the figure.

The overlapping broad bands in the 1200–970 cm^{-1} range resulted from Si—O—Si at the beginning changing to ν_3 P—O antisymmetric stretching vibrations at the end of an immersion. The peak at 963 cm^{-1} reflected the ν_1 P—O symmetric stretches. This peak is strongest in the TCP and weaker in the mineral of the test specimens. Carbonate groups (ν_2) also gave bands at 873–66 cm^{-1} in the HA and in the mineral of the test specimen. Band at 830 cm^{-1} is clearly seen in 0, 3 and 5 days immersion representing Si—OH groups. Two bands at 602 and 561-4 cm^{-1} represent ν_4 O—P—O bending vibrations of PO_4 groups in phosphate. These bands are dramatically strengthened as a function of immersion time. A phosphate ν_1 band is observed at 473 cm^{-1}. The peak is quite strong in the TCP and HA, and weaker in the specimen.

4. Discussion

In this study the inert E-glass fibers were impregnated with the bioresorbable PA, and further impregnated with the non-resorbable Bis-GMA-TEGDMA monomer system. After light polymerization and wet grinding of the specimens, these were immersed in the simulated body fluid for a maximum of 7 days. In the simulated body fluid the polymer of the PA dissolved immediately from the specimen, leaving open canals between the glass fibers and the non-resorbable matrix polymer, thus making it possible for the minerals to form in the canals. The thickness of the PA sizing in this study was so small that it did not allow enough space for bone ingrowth. However, the thickness of the PA sizing of the fibers can be increased to such as level that bone ingrowth into the "hollow cylindrical" canals is possible.

The mineral layer formed on the surface of the test specimen in one day investigated by SEM examination. The thickness of the mineral layer increased over time until 7 days when the layer was 18 μm thick. The attachment of the mineral layer to the surface of the specimens is probably only mechanical, and the cracking and loosening of the minerals from the surface of the test specimen occurring during the drying procedure after the mineralization took place. The test specimens that had not been immersed with the bioactive glass did not form a mineral layer on their surface due to the absence of the silica source. Hydrolyzed SiO_2-surface is known to be good nucleator of calcium phosphates [23, 24]. At body fluid and SBF pH = 7.4, the SiOH turns into anionic form SiO^- that adsorbs Ca^{2+} which in turn adsorbs phosphates. It may be possible that the E-glass fibers can promote the mineralization by acting as a substrate for nucleation. However, this could not be detected in this study mainly because of the slowly hydrolyzing Si—O—Si surface on the surface of the E-glass fibers.

The reference, the HA powder, was compressed into tablet-form before the EDX analysis for obtain the reference value for the Ca/P ratio (Ca/P = 1.68 ± 0.01) based on the theoretical calculations. When the HA powder was analyzed with the EDX, a large accumulation of charge within was found on the surface and the Ca/P ratio of 1.50 was quite far from the theoretical value. Thus, it can be assumed that to obtain the exact results based on the material's chemical formula from the EDX analysis, the surface of the materials should be quite smooth. Payne *et al.* also found this phenomenon in their study and concluded that the EDX analysis is only semi-quantitative method for measuring the Ca/P ratios of the different calcium phosphates [25]. For technical and material-based reasons, the surface of the test specimen with the fibers and the multiphase polymer matrix was so rough that variations were found in the Ca/P values. Moreover, the roughness and the shape of the mineral on the surface of the specimens varied among the groups BN, BEN and BESN, and even with in the groups some variations were found. This could influence the results of the Ca/P ratio. In this case, the standard deviations of the Ca/P ratios are high, making it difficult to draw conclusions. It is also possible that the mineral precipitation layer on the surface of the specimen was so thin that the X-ray beam could have penetrated to the polymer matrix, thus disturbing the analysis. In addition, the EDX analysis was made from

a relatively large area (about 11 mm^2), a fact that could also influence the results.

The FT-IR spectra of the synthetic commercial HA and TCP and the mineral on the surface of the test specimen indicate that there are some differences between the formed minerals and the HA/TCP. However, the IR spectra of the specimens treated with the bioactive glass (BN, BEN and BESN) were identical. Hydroxyl bands at 3571 and 630 cm^{-1} in the spectra of the specimens were masked by broad H_2O absorptions or no absorption peaks were detected because the specimens are amorphous. Phosphate bands at 561-4 and 602 cm^{-1} becomes stronger with time resembling eventually phosphate bands in the TCP and HA. At the same time the Si-OH band at 830 cm^{-1} became weaker. In the spectra of HA and TCP there were phosphate vibrations at 963 cm^{-1}, while this peak was not observed so clearly in the spectra of the specimens. The shape of the broad bands at the 1200–970 cm^{-1} change from Si—O—Si to phosphate group with time. Carbonate signals in the spectra of specimens at 1449 and 1415 cm^{-1} were changed with time resembling eventually carbonate signals in the spectra of TCP. Another carbonate peak of quite sharp shape or water was observed at 1635 cm^{-1} in the specimens immersed 0, 3 and 5 days but not in the 7 days immersion, TCP and HA. The carbonate moieties could be simply impurities, as found by Rehman [26], originating from the air, when they have been exposed to moisture and carbon dioxide or they could be from the SBF solution. The IR results indicate that the mineral on the surface of the specimen is mostly a mixture of HA and orthocalciumphosphate and other calcium phosphates, or it could be a calcium phosphate, which is evolving into HA. Although the HA is often desired for good osteoconductivity, the observed mixture of calcium phosphates could also be a benefit. The mixture of HA and TCP, i.e. biphasic calcium phosphate (BCP) [27], has a better bone-bonding ability than HA and can accelerate new bone formation [28]. Besides osteoconductivity, the BCP also has osteoinductive properties as a result of the micropores on its marcopore surface offering the possibility for endogenous bone morphogenetic protein to bind to it, and/or mild dissolution of the TCP from BCP ceramics, making it more active for bone formation than the HA [29]. Analogically, it has been suggested that imperfect, partly soluble HA of bone (with small crystal size, a lack of crystallinity and chemical imperfection) fulfills the need for normal biological resorption and redeposition of bone [30].

Because the presence of the bioactive glass seemed to be crucial for the apatite formation, the results of this study suggest that it might be indicated to add some bioactive glass to the fiber-reinforced composite, in the form of granules in the polymer matrix or as a fiber between the polymer matrix and the polymer PA dissolving silica for apatite formation. In the fiber-reinforced composite, all the fibers cannot be replaced with bioresorbable bioactive glass fibers because there should be a certain amount of reinforcing fibers in the composite in order to maintain adequate mechanical strength for surgical appliances.

5. Conclusions

Within the limitations of the study, the following conclusions can be drawn:

1. The surface of the fiber-reinforced composite with multiphase biopolymer matrix was mineralized by a biomimetic method using the bioactive glass as a silica source.
2. A layer of calcium and phosphorus precipitations is formed on the surface of the composites.
3. The IR and EDX analysis show that the mineral on the polymer surface is a calcium phosphate, but the exact form of it cannot be verified.
4. The mineral can penetrate into the canals formed between the glass fibers and the non-resorbable polymer matrix.

Acknowledgment

The National Technology Agency (TEKES) is gratefully acknowledged for financial support. The authors belong to the Bio- and Nanopolymer Research Group, which is a Center of Excellence (code number # 77317) funded jointly by the Academy of Finland and the National Technology Agency.

References

1. T. KOKUBO, *J. Ceram. Soc. Jpn.* **99** (1991) 965.
2. L. L. HENCH, *J. Am. Ceram. Soc.* **74** (1991) 1487.
3. T. PELTOLA, M. JOKINEN, H. RAHIALA, E. LEVÄNEN, J. B. ROSENHOLM, I. KANGASNIEMI and A. YLI-URPO, *J. Biomed. Mater. Res.* **44** (1999) 12.
4. S.-B. CHO, K. NAKANISHI, T. KOKUBO, N. SOGA, C. OHTSUKI, T. NAKAMURA, T. KITSUGI and T. YAMAMURO, *J. Am. Ceram. Soc.* **78**(7) (1995) 1769.
5. T. KOKUBO, *Biomaterials* **12** (1991) 155.
6. P. LI, X. YE, I. KANGASNIEMI, J. M. A. DE BLIECK-HOGERVORST, C. P. A. T. KLEIN and K. DE GROOT, *J. Biomed. Mater. Res.* **29** (1995) 325.
7. C. P. A. T. KLEIN, P. LI, J. M. A. DE BLIECK-HOGERVORST and K. DE GROOT, *Biomaterials* **16** (1995) 715.
8. K. HATA, T. KOKUBO, T. NAKAMURA and T. YAMAMURO, *J. Ceram. Soc.* **78** (1995) 1049.
9. M. TANAHASHI, T. YAO, T. KOKUBO, M. MINODA, T. MIYAMOTO, T. NAKAMURA and T. YAMAMURO, *J. Am. Ceram. Soc.* **77** (1994) 2805.
10. M. TANAHASHI, T. YAO, T. KOKUBO, M. MINODA, T. MIYAMOTO, T. NAKAMURA and T. YAMAMURO, *J. Appl. Biomater.* **5** (1994) 339.
11. F. MIYAJI, H.-M. KIM, S. HANDA, T. KOKUBO and T. NAKAMURA, *Biomaterials* **20** (1999) 913.
12. H. K. VARMA, K. SREENIVASAN, Y. YOKOGAWA and A. HOSUMI, *Biomaterials* **24** (2003) 297.
13. S. SAHA and S. PAL, *J. Biomed. Mater. Res.* **18** (1984) 435.
14. W. PETTY, *J. Biomed. Mater. Res.* **14** (1980) 427.
15. I.E. RUYTER and S. A. SVENDSEN, *J. Prosthet. Dent.* **43**(1) (1980) 95.
16. L. H. SPERLING, in "Over View of IPNs. Interpenetrating Polymer Networks" edited by D. Klempner, L.H. Sperling and L.A. Utracti (Advances in chemistry series: 239, American Chemical Society, Washington, DC, 1994) p. 4.
17. P. K. VALLITTU, *J. Prosthet. Dent.* **81**(3) (1999) 318.
18. P. K. VALLITTU and C. SEVELIUS, *J. Prosthet. Dent.* **84** (2000) 413.

19. Y. LIM, Y. H. CHOI and J. PARK, *J. Am. Chem. Soc.* **121** (1999) 5633.
20. M. VÄKIPARTA, M. KOSKINEN, P. K. VALLITTU, T. NÄRHI and A. YLI-URPO, *J. Mater. Sci. Mater. Med.* **15**(1) (2004) 69.
21. M. A. PUSKA, A. K. KOKKARI, T. O. NÄRHI and P. K. VALLITTU, *Biomaterials* **24** (2003) 417.
22. M. A. PUSKA, A. K. KOKKARI, T. O. NÄRHI, A. U. O. YLI-URPO and P. K. VALLITTU, *Appl. Comp. Mater.* **11** (2004) 17.
23. Ö. ANDERSSON, The bioactivity of silicate glass, Åbo Akademis kopieringscentral, Turku, 1990.
24. T. PELTOLA, Nanoscale Dimensions and *in vitro* Calcium Phosphate Formation: Studies on Sol-Gel-Derived Materials and Bioactive Glass (Annales Universitatis Turkuensis, Turku, 2000).
25. C. M. PAYNE and D. W. CROMEY, *J. Forens. Sci.* **35**(3) (1990) 560.
26. I. REHMAN and W. BONFIELD, *J. Mater. Sci. Mater. Med.* **8** (1997) 1.
27. R. Z. LEGEROS, S. LIN, R. ROHANIZADEH, D. MIJARES and J. P. LEGEROS, *J. Mater. Sci. Mater. Med.* **14** (2003) 201.
28. I. MANJUBALA, R. V. SURESH KUMAR and T. P. SASTRY, *Trends in Biomat. Artif. Org.* **14**(2) (2001) 27.
29. H. YUAN, M. VAN DEN DOEL, S. LI, C. A. VAN BLITTERWIJK, K. DE GROOT and J. D. DE BRUIJN, *J. Mater. Sci. Mater. Med.* **13** (2002) 1271.
30. A. POSNER, *Clin. Orthop.* **200** (1985) 87.

Received 11 March 2004
and accepted 11 March 2005